J. King Saud Univ., Vol. 4, Eng. Sci. (2), pp. 127-142 (1412 A.H./1992)

CHEMICAL ENGINEERING

Modelling and Simulation of Acrylonitrile Synthesis from Propylene Using Fluidized Bed Technology

A.H. Fakeeha, K.M. Wagialla and F.A. Al-Shriahy
Chemical Engineering Department, College of Engineering, King Saud University, P.O. Box 800, Riyadh 11421, Saudi Arabia
(Received 30/4/1991; Accepted for Publication 29/6/1991)

Abstract. The synthesis of acrylonitrile by the ammoxidation of propylene was modelled and simulated in a fluidized bed reactor based upon the two phase theory of fluidization. The conversion as obtained from two other models (the bubbling bed model and the bubble assemblage model) was calculated for comparison. The impact of the variation of each of four system parameters upon reactor performance was explored. A preliminary optimization search was initiated and it was shown that the model predicts a 76.6% conversion for a particular combinatioin of the four system parameters which compares favorably with the typical 60-65% conversion reported for actual industrial applications.

Nomenclature

A_b, A_w	:	Cross-sectional area of bubble phase and heat transfer area between bed and walls respectively, cm^2.
C_A	:	Concentration of reactant A, g.mole/cm^3.
C_{pg}	:	Gas heat capacity, J/g °C.
D_R	:	Reactor diameter, cm.
d_b, d_p	:	Bubble and particle diameters, cm.
H	:	Expaned bed height, cm.
$(H_{bd})_b$	:	Interface heat transfer coefficient between the bubble and dense phase, J/cm^3.sec.°C.
h_w	:	Bed to wall heat transfer coefficient, J/cm^2 K.
$(K_{bd})_{jb}$	:	Interphase mass transfer coefficient of component j between bubble and dense phase, sec^{-1}.

N_{jb}, N_{jd}, N_F : Molar flow rates of component j in bubble phase, component j in dense phase and total feed to reactor, gmol/sec.

P : Reactor pressure, atm.

Q_b, Q_d, Q_{dF}, Q_F : Gas volumetric flow rates in bubble phase, dense phase, feed to dense phase and total feed to reactor, cm^3/sec.

T_b, T_d, T_F, T_w : Temperatures of bubble phase, dense phase, feed and cooling medium, K.

U_b, U_0, U_{mf} : Superficial velocities of gas in bubble phase, fresh feed and at minimum fluidization, cm/sec.

V : Reactor volume, cm^3.

x_{jd}, x_{jF} : Mole fraction of component j in dense phase and feed respectively, dimensionless.

z : Bed height, cm.

α_j : Stoichiometric coefficient of component j in reaction, dimensionless.

δ : Bubble phase volume fraction, dimensionless.

ΔH_r : Heat of reaction, J/g.mol.

ρ_g, ρ_p : Density of gas and density of solid particles respectively, gm/cm^3.

$\varepsilon, \varepsilon_{mf}$: Dense phase voidage and dense phase voidage at minimum fluidization respectively, dimensionless.

γ_b : Ratio of solid disperssed in bubbles, dimensionless.

γ_c : Ratio of solid dispersed in clouds, dimensionless.

γ_e : Ratio of solid dispesed in emulsion, dimensionless.

K_{bc} : Interphase coefficient between bubble and cloud, m^3/sec.

K_{ce} : Interphase coefficient between cloud and emulsion, m^3/sec.

k_r : First order rate constant, s^{-1}.

Introduction

The major use of acrylonitrile today is in the manufacture of acrylic fibres. A wide variety of other uses include resins [particularly acrylonitrile -butadiene-styrene (ABS)], plastics, modified natural fibres, hydrolysed polymers as polyelectrolytes and as chemical intermediate.

For sometime now, the leading route to acrylonitrile has been by catalytic reaction of propylene with ammonia and air. The older process was based on either addition of HCN to acetylene or the addition of HCN to ethylene oxide, followed by the splitting off of a molecule of water. However, the ammoxidation propylene-based process uses relatively cheap feedstocks, and hence appears to have completely replaced the older processes for new construction worldwide. The process involves the premixing of three gaseous reactants and feeding them to the bottom of the fluidized bed reactor. Large size fluidized bed reactors are used which are provided with a top set of multiple effect cyclones for catalyst recovery as well as special sets of heat exchangers in the fluid bed for reaction heat removal and steam generation. The reactor effluent is scrubbed and the organic materials are recovered by distillation and absorption.

The vapour-phase reaction is according to the equation:

$$CH_2 = CH-CH_3+NH_3+1.5\,O_2 \rightarrow CH_2 = CH-C\equiv N+3H_2O \qquad (1)$$

Typical reaction temperatures are 420°C–500°C and pressures range from 1 to 3 atmospheres; feed composition ranges from 6.7-8 vol.% propylene, 7.5-9 vol. % ammonia and 82-86 vol. % air. A linear superficial gas velocity of 30-60 cm/sec and a contact time in the order of a few seconds are typically used [1]. The catalyst consists of oxygenated compounds of tellurium, cerium and molybdenum supported on silica particles. The average particle diameter is between 40-100 microns.

In this study a rigorous model based on the two phase theory of fluidization is presented for the acrylonitrile ammoxidation process in a fluidized bed reactor. A parametric sensitivity analysis is carried out to highlight the impact on reactor performance of the design and operating variables with a view to process optimization.

Model Development

The two phase theory of fluidization is used [2-6]. Allowance is made in this study for changes in gas volumetric flow rate in the dense phase due to reaction. Interphase mass transfer coefficients are calculated on a component-wise basis, (see Fig. 1).

It is assumed that the bubble gas is devoid of solids and is in plug flow. All the reaction occurs in the dense phase which is perfectly mixed and uniform in temperature. It is also assumed that the volumetric gas flow rate through the bubble phase is constant.

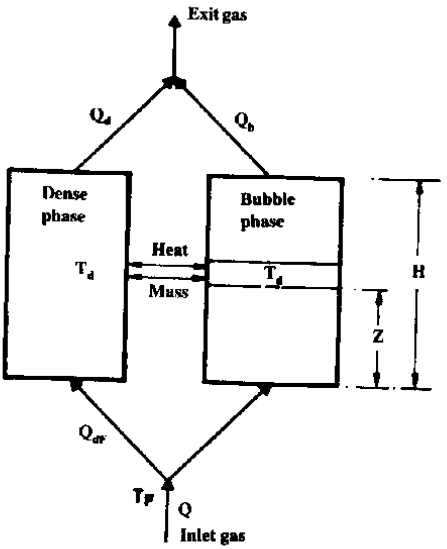

Fig. 1. Schematic diagram of fluidized bed reactor

Reaction mechanism and kinetics

The reaction mechanism, based on propylene ammoxidation, is given by equation (1). The kinetic model used was that reported by Gelbstein *et al.* [7] over bismuth-molybdate catalyst which is as follows:

$$r = 2.513 \exp\left(\frac{-16000}{RT}\right) p \qquad (2)$$

where

r = rate of disappearance of propylene to acrylonitrile in g. moles per second per gram of catalyst.

T = reaction temperature, K.

R = gas constant (82.06) cm^3 atm/gmol K.

p = partial pressure of propylene in atm.

Bubble phase material and energy balances

The steady state mass balance round an element of height Δz for the j^{th} component is given by:

$$\frac{dN_{jb}}{dz} = (K_{bd})_{jb} \left(\frac{N_{jb}}{Q_d} - \frac{N_{jb}}{Q_b}\right) A_b \tag{3}$$

An energy balance gives:

$$\rho_g \, C_{pg} \, u_b \, \frac{dT_b}{dz} = (H_{bd})_b \, (T_d - T_b) \tag{4}$$

Dense phase material and energy balances

For component j in the dense phase, the molar flow rate is given by:

$$N_{jd} = N_{jdF} + \int_0^H (K_{bd})_{jb} \left(\frac{N_{jb}}{Q_d} - \frac{N_{jd}}{Q_b}\right) \text{——} A_b dz + V(1-\delta)(1-\varepsilon)\rho_p a_j r \tag{5}$$

The integral in equation (5) is obtained analytically from the bubble phase equation (equation 3). Rearranging equation (3) and integrating (noting that $N_{jb} = N_{jbF}$ at $z = 0$) we obtain

$$\left(\frac{N_{jb}}{Q_b} - \frac{N_{jd}}{Q_d}\right) = \left(\frac{N_{jbF}}{Q_b} - \frac{N_{jd}}{Q_d}\right) e^{-a_j z} \tag{6}$$

where

$$a_j = (K_{bd})_{jb} / u_b \tag{7}$$

where $(K_{bd})_{jb}$ is the interphase mass transfer coefficient between bubble and dense phase on bubble volume and is given by the correlation [8]:

$$\frac{1}{(K_{bd})_{jb}} = \frac{1}{(K_{bc})_{jb}} + \frac{1}{(K_{cd})_{jb}} \tag{8}$$

where

$$(K_{bc})_{jb} = 4.5 \left(\frac{u_{mf}}{d_B}\right) + 5.85 \left(\frac{D_{jm}^{1/2} \, g^{1/4}}{d_B^{5/4}}\right) \tag{9}$$

$$(K_{cd})_{jb} = 6.78 \left(\frac{\varepsilon_{mf} \, D_{jm} \, u_b}{d_B^3}\right)^{1/2} \tag{10}$$

D_{jm} is the diffusivity of component j in the gas mixture and is given by the correlation [9]:

$$D_{jm} = \frac{(1 - x_j)}{\left[\sum_{\substack{i=1 \\ i \neq j}}^{n} \left(\frac{x_j}{D_{ji}}\right)\right]} \tag{11}$$

D_{ij} is the binary diffusivity and is given by the correlation [10]:

$$D_{ij} = 0.04357 \frac{T^{3/2}}{P(V_i^{1/3} + V_j^{1/3})^2} \sqrt{\frac{1}{M_i} + \frac{1}{M_j}} \tag{12}$$

u_b in equation (7) represents the bubble rising velocity and is correlated by the expression [8]:

$$u_b = u_0 - u_{mf} + (g d_B)^{0.5} \tag{13}$$

u_0 is the superficial gas velocity. u_{mf} is the superficial gas velocity at minimum fluidization and is correlated as follows [10]:

$$u_{mf} = 0.01 \left(\frac{\mu}{\rho_g d_p}\right) \left(\sqrt{27.2^2 + 0.0408 A_r} - 27.2\right) \tag{14}$$

where A_r is the Archimedes number. The bubble diameter in equation (13) is given by the correlation [11]:

$$d_B = d_{BM} - (d_{BM} - d_{B0}) \exp(-0.3 z/D) \tag{15}$$

where

$$d_{BM} = 411.38 [A (u_0 - u_{mf})]^{0.4} \tag{16}$$

$$d_{B0} = 0.376 (u_0 - u_{mf})^2 \tag{17}$$

$$\frac{N_{jbF}}{Q_b} = \frac{N_{jF}}{Q_F} \tag{18}$$

Then

$$\left(\frac{N_{jb}}{Q_b} - \frac{N_{jd}}{Q_d}\right) = \left(\frac{N_{jF}}{Q_F} - \frac{N_{jd}}{Q_d}\right) e^{-\alpha_j z} \tag{19}$$

Substituting equation (19) into equation (5) and intergating we obtain:

$$N_{jd} = N_{jdF} + u_b A_b \left(\frac{N_{jF}}{Q_F} - \frac{N_{jd}}{Q_d}\right)(1 - e^{-a_j H}) + V(1-\delta)(1-\varepsilon)\ \rho_p\ \alpha_j r \tag{20}$$

For ideal gas law we obtain:

$$x_{jd}\ P\ Q_d = N_{jd}\ R\ T_d \tag{21}$$

$$x_{jF}\ P\ Q_F = N_{jF}\ R\ T_F \tag{22}$$

$$N_{jdF} = x_{jF}\ N_F\ (Q_{dF} / Q_F) \tag{23}$$

Equation (9) now becomes:

$$N_{jd} = x_{jF} N_F \left(\frac{Q_{dF}}{Q_F}\right) + \frac{P u_b\ A_b}{R}\left(\frac{x_{jF}}{T_F} - \frac{x_{jd}}{T_d}\right)(1 - e^{-a_j H}) + V(1-\delta)(1-\varepsilon)\ \rho_p\ a_j r \tag{24}$$

Similarly the bubble phase energy balance is integrated analytically to yield

$$T_b = T_d - (T_d - T_F)\ e^{-bz} \tag{25}$$

where

$$b = H_{bd} / u_b\ \rho_g\ C_{pg} \tag{26}$$

$(H_{bd})_b$ is the overall heat transfer coefficient (bubble-phase to dense-phase) based on bubble volume and is correlated as follows [8]:

$$\frac{1}{(H_{bd})_b} = \frac{1}{(H_{bc})_b} + \frac{1}{(H_{cd})_b} \tag{27}$$

where

$$(H_{bc})_b = 4.5 \left(\frac{u_{mf}\ \rho_g\ C_{pg}}{d_B}\right) + 0.104 \left(\frac{k_g\ \rho_g\ C_{pg}}{d_B^{2.5}}\right)^{1/2} \quad (28)$$

$$(H_{cd})_b = 21.44\ (k_g\ \rho_g\ C_{pg})^{1/2} \left(\frac{\varepsilon_{mf}\ u_b}{d_B}\right)^{1/2} \quad (29)$$

The energy balance equation then becomes

$$\rho_g\ C_{pg}\ Q_{dF}\ (T_F - 298) - \rho_g\ C_{pg}\ Q_d\ (T_d - 298)$$

$$+ \int_0^H (H_{bd})_b\ (T_b - T_d)\ A_b dz + h_w\ A_w\ (T_w - T_d)$$

$$+ V(1 - \rho)\ (1 - \varepsilon)\ \rho_p\ (-\Delta H)\ r = 0 \quad (30)$$

where h_w is the heat transfer coefficient (bed to cooling surface) and is correlated by the expression [12]:

$$h_w = 0.88\ (k_g / d_p)\ A_r^{0.213} \quad (31)$$

Substituting for T_b from equation (25) and integrating we obtain:

$$\rho_g\ C_{pg}\ Q_{dF}\ (T_F - 298) - \rho_g\ C_{pg}\ Q_d\ (T_d - 298) +$$

$$u_b\ \rho_g\ C_{pg}\ A_b\ (T_F - T_d)\ (1 - e^{-bH}) + h_w\ A_w\ (T_w - T_d) +$$

$$V(1 - \rho)\ (1 - \varepsilon)\ \rho_p\ (-\Delta H)\ r = 0 \quad (32)$$

Computational Procedures

The material and energy balance can be decoupled in computer calculations. The set of non-linear simultaneous algebraic equations (6) were solved by the Newton-Raphson technique. The temperature at which equation (32) is satisfied represents a steady state operating temperature. For this purpose, a heat function (defined in equation (33) below) is zero at steady state temperature.

$$\text{Heat function} = \rho_g\ C_{pg}\ Q_{dF}\ (T_F - 298) - \rho_g\ C_{pg}\ Q_d\ (T_d - 298)$$

$$+ u_b \rho_g C_{pg} A_b (T_F - T_d)(1 - e^{-bH}) + h_w A_w (T_w - T_d)$$

$$V (1 - \delta)(1 - \varepsilon) \rho_p (- \Delta H) r \qquad (33)$$

Results and Discussion

Table 1 shows the design and operating data of the base case.

Table 1. Design and operating data of the base case

Reactor diameter (cm)		400
Static bed height (cm)		800
Catalyst particle diameter (μm)		100
Bed voidage at minimum fluidization (ε_{mf})		0.367
Min. Fluid Vel. (U_{mf})		14.13 cm/sec
Superficial gas vel. (U_0)		49.77 cm/sec
Feed temperature		300 K
Feed composition in mol %		
propylene	7.3 %	
ammonia	8.2 %	
air	84.5 %	
Pressure		2 atm.

Due to lack of industrial plant data for validation of model accuracy, the conversion as predicted by the model was compared against the conversions predicted by two other well known models; the Bubble Bed Model [8] and the Buble Assemblage Model [13]. As shown in Tables 2 and 3 comparable results were obtained.

The differences in results are due to the basic assumptions of each model. The Bubbling Bed Model (also known as the Kunii-Levenspiel model) differs from the two phase model in that the former assumes a cloud-wake region surrounding the rising bubbles in which gas-solid reaction occurs and it also allows for inter-phase gas transfer in two consecutive stages between bubble and cloud-wake and between cloud-wake and dense phase [14, p.60]. The two phase model allows for two factors ignored by the bubbling bed model and these are bubble growth and reaction in the dense phase. The bubbling bed model gives the fraction of reactant leaving the bed surface unreacted (for a first order reaction) as:

$$\frac{C_A}{C_{A0}} = \exp (1 - k_f) \qquad (34)$$

where

Table 2. Bubble bed model

Bed voidage (ε_{mf})	= 0.367
Operating velocity (cm/sec)	= 49.77
Min. fluid. velocity (cm/sec)	= 5.33
Effective bubble diameter (cm)	= 103
Static bed height (cm)	= 800
Reaction constant (1/sec)	1.964
Effective diffusivity (cm^2/sec)	0.258
K_{bc} (bubble-cloud) (1/sec)	= 0.2833867
K_{ce} (cloud-emulsion) (1/sec)	= 3.281442E-02
Vol. of wake/vol. of bubble (alpha)	= 0.34
Vol. of solid in bubble/vol of bubble	= 0
Vol. of solid in cloud & wakes/vol. of bub	= 0.3457335
Vol. of solid in emulsion/vol. of bubble	= 2.871951
Propylene conversion (%)	= 51.23

Table 3. Bubble assemblage model

Particle diameter (cm)	= 0.01
Bed voidage (ε_{mf})	= 0.367
Min. fluid.. velocity (cm/sec)	= 5.33
Operating velocity (cm/sec)	= 49.77
Reaction constant (1/sec)	= 1.964
Fractional volume change on complete conversion	= 1.6
Incipient fluidized height (cm)	= 800
Expanded bed height (cm)	= 1107.787
Number of stages	= 10
Propylene conversion (%)	= 55.09

$$k_f = \frac{H\ k_r}{U_b}\left[\gamma_b + \frac{1}{\dfrac{k_r}{k_{bc}} + \dfrac{1}{\dfrac{k_r}{k_{ce}} + \dfrac{1}{\gamma_e}}}\right]$$

The model is particularly sensitive to the estimated value of bubble diameter d_b

The bubble assemblage model allows for variation of bubble size with bed height. The initial bubble diameter at the distributor is calculated from a correlation and the bed is then divided into a number of vertical compartments whose height is equal to the bubble diameter at the corresponding bed height. The reactant gas is assumed to be prefectly mixed in the bubble and dense phases. Overall conversion is calculated by a stagewise solution of the mass balance equations [13,14].

It is noteworthy that the two phase model as presented in this paper is more general in its applicability than the Bubbling Bed and Bubble Assemblage models in that it can handle multiple reactions as well as complex kinetics whereas the two models referred to earlier can handle only single reaction, first order kinetics.

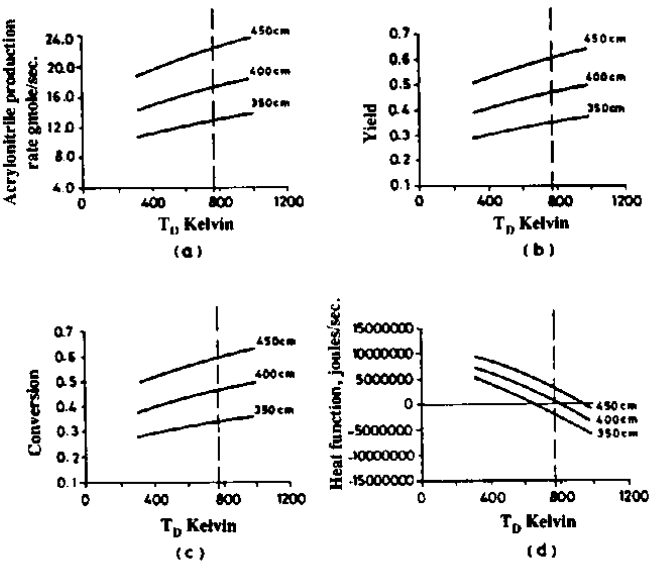

Fig. 2. Effect of reactor diameter variation on

a) Acrolynitrile production
b) Yield
c) Conversion
d) Heat function

The system performance was then evaluated according to three performance criteria; conversion, yield and acrylonitrile production rate. The parametric sensitivity analysis was carried out by imposing changes in two design variables (reactor diameter and particle size) and two operating variables (pressure and feed compos-

ition). Fig. 2 shows the effect of the variation of the reactor diameter (for the same gas feed rate) on heat function, conversion, yield and acrylonitrile production rate. It is noteworthy that an increase in reactor diameter in this case is equivalent to a decrease in superficial gas velocity (U_0). As is shown in Fig. 2a, the steady state temperature for the base case of D_R = 400 cm is about 790 K. A decrease in D_R to 350 cm makes it possible to operate at T_D = 650 K but at a much lower conversion (of about 33%) yield and production rate (see Figs. 2b, 2c and 2d). For the same gas feed flow rate, operation with a 450 cm diameter reactor makes it possible to attain a conversion of about 63% (because of a decreased U_0 and hence a smaller bubble diameter d_B) but the operating temperature in this case (which is over 950 K) (see Fig. 2a) might not be practically desirable.

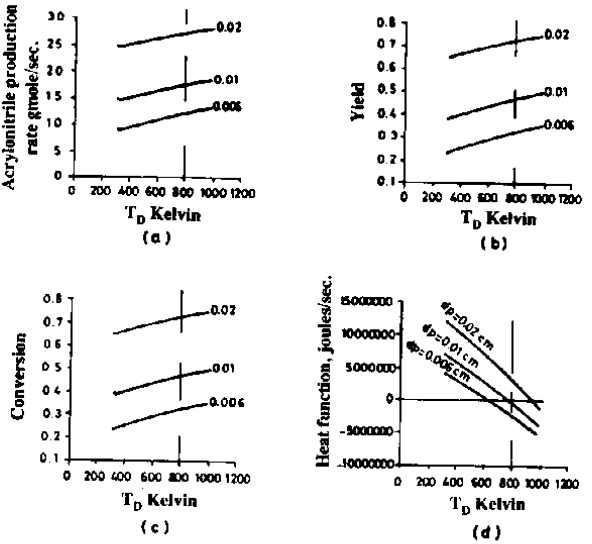

Fig. 3. Effect of particle size variation on

a) Acrolynitrile production
b) Yield
c) Conversion
d) Heat function

Figure 3 shows the effect of variation of particle size from the base case of d_p = 100 μm to 60 μm and 200 μm. It is clear from Fig. 3 that reduction of particle size is not compatible with enhanced system performance. However, the use of a particle diameter of 200 μm resulted in a conversion of over 73.7% albeit at an elevated temperature of 950 K.

Figure 4 shows the effect of the variation of pressure from the base case of 2 atm to 1 atm and 3 atm. When the operating pressure is 1 atm, the steady state conversion becomes 26% and the production rate 9.54 gmole/sec only at temperature of 950 K. Operation at 3 atm resulted in a conversion of 61% and a production rate of 22.43 gmole/sec at a temperature 890 K. Thus the higher pressure operation is advantageous provided that the high temperature that goes with it does not result in product cracking or in catalyst destruction.

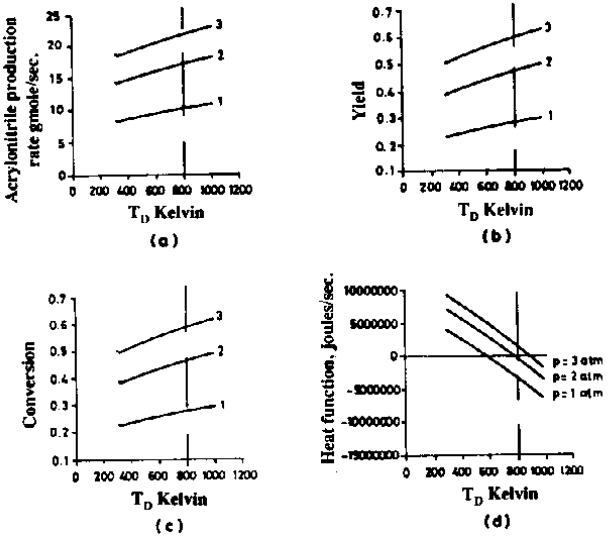

Fig. 4. Effect of pressure variation on

a) **Acrolynitrile production**
b) **Yield**
c) **Conversion**
d) **Heat function**

Figure 5 shows the effect of the variation of feed composition from the base case as follow is (in mole %):

	Case 1 (Base case)	Case 2	Case 3
Propylene	7.3	5.0	9.0
Ammonia	8.2	7.5	14.5
Air	84.5	87.5	76.5

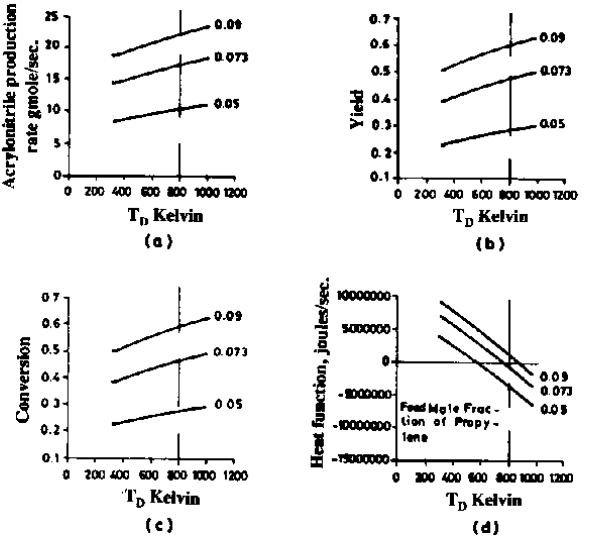

Fig. 5. Effect of feed composition on

a) Acrolynitrile production
b) Yield
c) Conversion
d) Heat function

As shown in Fig. 5 the conversion and yield are both about 47% for the base case and the production rate is 17.27 gmoles/sec. A decrease in reactants feed concentration as in case 2 reduces the conversion and yield to 44% and production rate to 11.23 gmoles/sec at an operating temperature of 630 K. Increasing the reactant feed concentrations (case 3) results in improvements in conversion, yield and production rate to 49% and 22.27 gmoles/sec respectively. However, the operating temperature is a very high one at about 930 K.

A sub-optimal reactor design and operational configuration was undertaken by changing each of the four parameters examined so far in favourable directions. For a bed diameter of 425 cm, a particle diameter of 150 μm, a pressure of 2.5 atmospheres and a feed concentration of 8% propylene, 12% ammonia and 80% air, it is possible to achieve a conversion of 76.6%, a yield of 76.4% and a production rate of 31.08 g.moles/sec. In terms of the production rate this represents a 84% improvement over the base case. Typical industrial conversions are in the 60-65% range. Due to excessive heat generation by reaction in the optimized set-up, the heat removal rate must be increased by 150% in order to operate at a reasonable steady state tem-

perature of 750 K. This increased heat removal rate may be achieved by increasing the heat transfer area, and/or decreasing the feed temperature. A computer-aided multivariable optimization search is now under study for overall optimization of reactor performance.

Conclusion

A rigorous physically-based model to simulate a fluidized bed reactor was developed for acrylonitrile production by ammoxidation. A parametric sensitivity analysis of four variables (D_R, d_p, pressure and feed composition) was carried out. An optimization exercise was then undertaken which enabled production rate to be improved by 84% by an expeditious variation of each of these parameters as well as the cooling rate.

References

[1] Caporali, G. "How Montedison Makes Acrylo." *Hydrocarbon processing*, 51, No. 11 (1972), 144-146.

[2] Toomy, R.D. and Johnstone, H.F. "Gas Fluidization of Solid Particles." *Chem. Engng Prog.*, No. 48 (1952), 220.

[3] Werther, J. "Mathematical Modeling of Fluidized Bed Reactor." *International Chemical Engineering*, 20, No. 4 (1981), 529-541.

[4] Wagialla, K.M.; Elnashaie, S.S. and Fakeeha, A.H. "Review on Heat Transfer in Gas Solid Fluidized Beds." *J. King Saud Univ.*, Vol. 2, *Eng. Sci.* 2, (1990), 331-346.

[5] Elnashaie, S.S.; Wagialla, K.M. and Abashar, M.E., "Fluidized Bed Reactor for Ammonia Synthesis – Preliminary Theoretical Investigation." Accepted for publication in *Mathematical and Computer Modelling* (1991).

[6] Wagialla, K.M.; Helal, A.M. amd Elnashaie, S.S.E.H. "The Use of Mathematical and Computer Models to Explore the Applicability of Fluidized Bed Technology for Highly Exothermic Catalytic Reactions I. Oxidative Dehydrogenation of Butene," Accepted for publication in *Mathematical and Computer Modelling* (1990).

[7] Gelbstein, A.I.; Bakshi, Yn. Stroeva, S.S.; Kulkovva, N.V.; Lapidus, V.I. and Sadovski, A.S. "The Study of Bismuth-Molybednum Catalysts for the Partial Oxidation and Oxidative Ammonolysis of Propylene." *Kinetics and Catalysis (USSR) (Engl. Trans.)*, 6, No. 6 (1965), 927-933.

[8] Kunii, D. and Levenspiel, O. *Fluidization Engineering*. New York: J. Wiley, 1977.

[9] Reid, R.C.; Prausnitz, J.M. and Sherwood, T.K. *The Properties of Gases and Liquids*. 3rd Edition. New York: McGraw-Hill Book Company, 1977.

[10] Coulson, J.M. and Richardson, J.F. *Chemical Engineering*, Vol. 1. Oxford: Pergamon Press, 1965.

[11] Mori, S. and Wen. C.Y. "Estimation of Bubble Diameter in Gaseous Fluidized Beds." *AIChEJ*, 21 (1975), 109-115.

[12] Renz, U. "Heat Transfer Characteristics of the FBC at Acchen Technical University," *Proceedings of the 1987 Internatiuonal Conference on Fluidized Bed Combustion*, American Society of Mechanical Engineers, N.Y. (1987).

[13] Wen, C.Y. and Fan, L.T. *Models for Flow Systems and Chemical Reactors*. New York: Marcel Dekker Inc., 1975.

[14] Doraiswamy, L.K. and Kulkarni, B.D. *Transport Processes in Fluidized Bed Reactors*. New Delhi: Wiley Eastern Limited, 1987.

نمذجة ومحاكاة تصنيع الأكرونتريل من البروبيلين باستخدام تقنية المهد المميَّعة

أنيس حمزة فقيها، كامل محمد الحسن وقيع الله و فهد الشريهي

قسم الهندسة الكيميائية، كلية الهندسة، جامعة الملك سعود، ص. ب ٨٠٠، الرياض ١١٤٢١، المملكة العربية السعودية

(استلم في ١٩٩١/٤/٣٠م، قبل للنشر في ١٩٩١/٦/٢٩م)

ملخص البحث. لقد تمت نمذجة ومحاكاة تصنيع الأكرونتريل بأكسدة البروبيلين في وجود الأمونيا في مفاعل ذي مهد مميعة باستخدام نموذج ثنائي الطور. كما تمَّ حساب مقدار التحول باستخدام نموذجين آخرين (نموذج المهد ذي الفقاقيع، ونموذج تجميع الفقاقيع) للمقارنة. وقد تمت دراسة أثر تغير أربعة متغيرات على أداء المفاعل. وقد دلَّت دراسة مبدئية للبحث عن الوضع الأمثل على أن النموذج الرياضي المستخدم يشير إلى أن هناك قيمًا معيَّنة للمتغيرات الأربعة تحقق تحولاً قدره ٧٦,٦٪ مقارنة بالتحول المعلن في التطبيقات الصناعية وهو ٦٠ ـ ٦٥٪.